Conformation and Crystal Structure of Poly(α-cycloalkyl-*β*-L-aspartate)s

Montserrat García-Alvarez, Antxon Martínez de Ilarduya, Salvador León, Carlos Alemán, and Sebastián Muñoz-Guerra*

Departament d'Enginyeria Química, Universitat Politècnica de Catalunya, E.T.S. d'Enginyers Industrials, Diagonal 647, Barcelona E-08028, Spain

Received: October 17, 1996; In Final Form: March 19, 1997[⊗]

The conformation and crystal structure of two nylon 3 derivatives bearing a cycloalkoxycarbonyl group on the *β*-carbon of the main chain, namely, poly(α-cyclopentyl-*β*-L-aspartate) and poly(α-cyclohexyl-*β*-L-aspartate), were examined. X-ray diffraction data revealed that both compounds adopt a 13/4 helical conformation of the type usually found for the hexagonal form of poly(*β*-L-aspartate)s bearing acyclic alkyl side chains. Whereas poly(α-cyclopentyl-*β*-L-aspartate) crystallized in a monoclinic structure (pseudohexagonal, space group $P2_1$), the cyclohexyl derivative deviated from the general pattern, crystallizing in a slightly distorted hexagonal lattice in the space group *P*1. AMBER energy optimization algorithms and linked-atom least-squares refinement applied to X-ray data were used to analyze the structure of poly(α-cyclohexyl-*β*-L-aspartate). Energy calculations made on an isolated chain revealed that the cyclohexyl side group is in the equatorial chair conformation and that the 13/4 helix will be sterically incompatible with the existence of mixed populations of axial and equatorial conformers within the same molecule. The analysis of the mimicked crystal favored the antiparallel arrangement of chains, but it was unable to discriminate between the different crystal models compatible with diffraction data. ^{1}H NMR measurements in solution proved that the helical conformation adopted in the solid state is still retained in the liquid state. ^{13}C CP−MAS NMR experiments furnished further evidence on the structural conclusions derived from theoretical methods.

Introduction

During the last decade a good amount of effort has been devoted to the study of poly(α-alkyl-*β*-L-aspartate)s,[1−4] a family of nylon 3 derivatives showing exceptional interest due to their ability to adopt helical conformations with features similar to the well-known α-helix of polypeptides and proteins. These stereoregular polyamides have the following repeating unit,

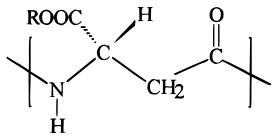

where R is an alkyl group containing from 1 to 22 carbon atoms. The knowledge accumulated on the structure of these substances has made it possible to advance far in the rationalization of the relation existing between the size of the alkyl side group and the conformation and mode of packing assumed by the polymer in the solid state. A pseudohexagonal lattice made of up-and-down right-handed helices with 13 residues per four turns is the usual structure adopted by poly(*β*-L-aspartate)s.[5−8] Deviation from this general pattern occurs however for members with alkyl side chains of extreme sizes. Thus, a 17/4 helix seems to be the conformation present in the hexagonal form of both the methyl and ethyl derivatives,[9] and a layered structure of 13/4 helices with side chains filling the interlayer space is adopted by members bearing alkyl groups containing 12 or more carbon atoms.[8] A rather ambiguous structural behavior is displayed by the hexyl and octyl derivatives in consonance with the length of their respective side groups.[8,10]

Polymorphism is frequent in poly(*β*-L-aspartate)s.[11] A second tetragonal form composed of right-handed 4/1 helices is observed for members with ethyl, propyl, and butyl side chains. Furthermore extended chain conformations of *β*-pleated sheet type are found in addition for both the methyl and the ethyl derivatives.[9] The influence of side group interactions on the conformational preferences displayed by poly(*β*-L-aspartate)s has been examined in some detail.[12,13] Large linear alkyl groups seem to be incompatible with the tetragonal form due to the poor efficiency attainable in the packing of the chains. Conversely, branched alkyl groups of medium size appear to favor this form because (i) they may fill efficiently the intermolecular space and (ii) favorable intramolecular interactions take place among them when the polymer is arranged in a 4/1 helical conformation.

No poly(*β*-L-aspartate) bearing alicyclic side groups has been investigated thus far. In this work we report on the crystal structure of poly(α-cyclopentyl-*β*-L-aspartate) and poly(α-cyclohexyl-*β*-L-aspartate), abbreviated PACPLA and PACHLA, respectively. The interest driving this study is double. On one side, and in line with preceding investigations, it would be desirable to know if the conformation and mode of packing of poly(*β*-L-aspartate)s are influenced by the cyclic nature of the side chain. In the case of the cyclohexyl group this study is particularly tempting due to the effect that the axial−equatorial chair equilibrium may have on the stability of the helix. As a matter of fact, photoinduced *cis*−*trans* changes taking place in the side chain of certain poly(α-L-aspartate)s are known to provoke the transition of the main chain from α-helix to random coil conformation.[14,15] On the other hand it is of interest also to examine the effect exerted by the helix on the axial−equatorial chair equilibrium of the cyclohexyl group. In part 1 of this work,[16] a conformational study of compound (*S*)-4-(cyclohexoxycarbonyl)-2-azetidinone, which is the monomer used in the manufacture of PACHLA, was carried out. Results obtained thereof concerning the structure of the cyclohexyl group led to the conclusion that the equatorial conformation is largely favored in solution and that such preference is not

* To whom correspondence should be sent.
⊗ Abstract published in *Advance ACS Abstracts,* May 1, 1997.

S1089-5639(96)03208-2 CCC: $14.00

TABLE 1: Data of Poly(α-cycloalkyl-*β*-L-aspartate)s Studied in This Work

	viscosity data		thermal data		
polymer	$[\eta]$ (dL g^{-1})[a]	$M_v \times 10^{-5}$ [b]	T_m (°C)[c]	T_d (°C)[d]	ρ (g mL^{-1})[e]
PACPLA	1.22	2.2	300	297/376	1.09
PACHLA	1.53	2.8	315	308/371	1.18

[a] Intrinsic viscosity measured in dichloroacetic acid at 25 °C. [b] Averaged molecular weight estimated by applying the equation reported for poly(γ-benzyl-α-L-glutamate).[20] [c] Melting temperature measured by DSC. [d] First and second decomposition temperatures measured by TGA. [e] Density measured by the flotation method in aqueous solutions of KBr.

significantly affected by the polarity of the solvent. The knowledge gained about the structural behavior of the monomer will be of great assistance in the interpretation of the results that we have obtained in the conformational analysis of the polymer.

Experimental Section

Materials. The two poly(α-cycloalkyl-*β*-L-aspartate)s (PACPLA and PACHLA) used in this work were prepared by nonassisted anionic ring-opening polymerization of the optically pure (*S*)-4-(cyclopentoxycarbonyl)-2-azetidinone and (*S*)-4-(cyclohexoxycarbonyl)-2-azetidinone, respectively. The synthesis of these monomers from L-aspartic acid has been reported in full detail elsewhere,[17] and the methodology used for polymerization is that generally applied in the preparation of poly(α-alkyl-*β*-L-aspartate)s.[18−19] In brief, a solution of the monomer in dimethyl sulfoxide (18% w/w) containing sodium pyrrolidone (0.4% w/w) is left to stand under stirring at room temperature for 24 h. The polymer is recovered from the reaction mixture by precipitation with methanol and purified by repeated precipitation with methanol from $CHCl_3$−TFA solutions. Some characterization data of PACHLA and PACPLA of relevance to the accomplishment of the present study are given in Table 1.

Poly(α-cyclopentyl-*β*-L-aspartate). From 1.0 g of (*S*)-4-(cyclopentoxycarbonyl)-2-azetidinone 0.81 g of polymer was obtained. Elemental anal. Calcd for $C_9H_{13}NO_3$: C, 59.00; H, 7.15; N, 7.64. Found: C, 58.75; H, 6.92; N, 7.89. IR (cm^{-1}, film cast from TFA): 3288 (NH, amide A), 3088 (amide B), 1738 (ester C═O), 1659 (amide I), 1550 (amide II). ^{1}H NMR ($CDCl_3$/TFA), δ (ppm): 8.0 (d, 1H, N*H*), 5.27 (m, 1H, COOC*H*), 4.85 (m, 1H, α-C*H*), 3.12 (m, 2H, *β*-CH_2), 1.88 (m, 4H, COOCHCH_2), 1.69 (m, 4H, COOCHCH$_2$CH_2). ^{13}C NMR ($CDCl_3$/TFA), δ (ppm): 173.44 (*C*ONH), 173.06 (*C*OO), 83.02 (COO*C*H), 50.59 (NH*C*H), 37.25 (*C*H$_2$CO), 32.94 (COOCH*C*H$_2$), 24.18 (COOCHCH$_2$*C*H$_2$).

Poly(α-cyclohexyl-*β*-L-aspartate). From 1.0 g of (*S*)-4-(cyclohexoxycarbonyl)-2-azetidinone, 0.86 g of polymer was obtained. Elemental anal. Calcd for $C_{10}H_{15}NO_3$: C, 60.90; H, 7.67; N, 7.10. Found: C, 60.69; H, 7.64; N, 7.20. IR (cm^{-1}, film cast from TFA): 3287 (NH, amide A), 3089 (amide B), 1742 (ester C═O), 1656 (amide I), 1550 (amide II). ^{1}H NMR ($CDCl_3$/TFA), δ (ppm): 7.97 (d, 1H, N*H*), 4.81 (m, 2H, COOC*H* and α-C*H*), 3.04 (m, 2H, *β*-CH_2), 1.75 (m, 4H, COOCHCH_2), 1.51 (m, 4H, COOCHCH$_2$CH_2), 1.31 (m, 2H, COOCHCH$_2$CH$_2$CH_2). ^{13}C NMR ($CDCl_3$/TFA), δ (ppm): 172.61 (*C*ONH), 171.79 (*C*OO), 77.52 (COO*C*H), 49.88 (NH*C*H), 36.63, (*C*H$_2$CO), 31.11 (COOCH*C*H$_2$), 25.11 (COOCHCH$_2$CH$_2$*C*H$_2$), 23.48 (COOCHCH$_2$*C*H$_2$).

Measurements. Microanalyses were performed by Servei de Microanàlisi (CSIC, Barcelona). Viscosities were determined in dichloroacetic acid solution at 25 °C using a Ubbelhode microviscometer. Densities were measured by the flotation method in aqueous KBr solutions. Infrared spectra were registered on a Perkin-Elmer 2000 FTIR instrument from thin films prepared by casting in trifluoroacetic acid. Thermal measurements were made on a Mettler TA-400 thermoanalyzer at a scanning rate of 10 K min^{-1} under a nitrogen atmosphere. X-ray diffraction diagrams were obtained on flat films in a modified Statton camera (W. Warhus, Wilmington, DE) using nickel-filtered copper radiation of wavelength 1.542 Å and calibrated with molybdenum sulfide (d_{002} = 6.147 Å). ^{1}H (300.13 MHz) and ^{13}C (75.5 MHz) NMR spectra were registered on a Bruker AMX-300 instrument equipped with a CP−MAS accessory and a variable-temperature unit. Spectra from solution were taken at 25 °C with the sample dissolved in deuterated chloroform containing variable amounts of trifluoroacetic acid and using tetramethylsilane (TMS) as internal reference. Solid-state ^{13}C CP−MAS NMR spectra were acquired in the −70 to +80 °C temperature range using sample 50−100 mg weights, which were spun at 2.0−4.0 kHz in a cylindrical ceramic rotor. Contact and repetition times of 2 ms and 10 s were used, and the number of transients accumulated for each spectrum was between 256 and 5000. The spectral width was 31.2 kHz, and the number of data points was 4K. Chemical shifts were externally calibrated against the higher field peak of adamantane appearing at 29.5 ppm relative to TMS.

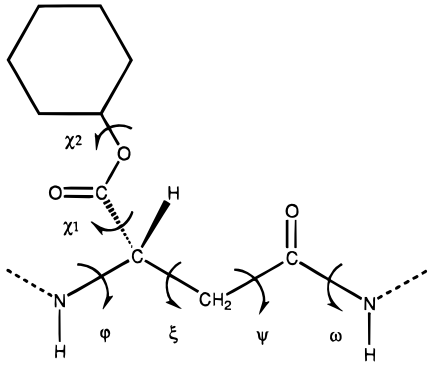

Figure 1. Schematic representation of the monomeric unit of PACHLA with indication of the torsion angles.

Energy Calculations. These calculations were performed with the AMBER 3.0 rev. A program[21] with explicit consideration of all atoms. The electrostatic charge distribution on the backbone and the parameters for the bonding terms of the ester side group were those previously used in the study of other related poly(α-alkyl-*β*-L-aspartate)s.[12,13] Side chain atoms were parametrized according to a methodology developed by us and reported elsewhere.[23,24] A schematic representation of the monomeric unit of PACHLA with indication of the torsion angles considered in the conformational analysis is shown in Figure 1. Energy optimizations were carried out in two steps. Firstly, the most unfavorable interactions were removed by a steepest descent optimization. Secondly, the conformation was optimized until the energy difference or the norm of the gradient for two successive optimizations was less than 10^{-7} or 0.1 kcal mol^{-1} residue, $^{-1}$ respectively. An environment with a dielectric constant $\epsilon = 1$ was assumed, 1−4 interactions were scaled to 0.5, and nonbonding interactions were cut off at 8 Å.

The starting models were right-handed 13/4 helices constructed with the conformational parameters available for the standard 13/4 helix of poly(*β*-L-aspartate)s.[13] Geometry optimizations were made by molecular mechanics minimization of the conformational energy. Firstly the conformation of an isolated chain was optimized, and then the analysis was extended to a set of 12 chains mimicking the crystal environment. The

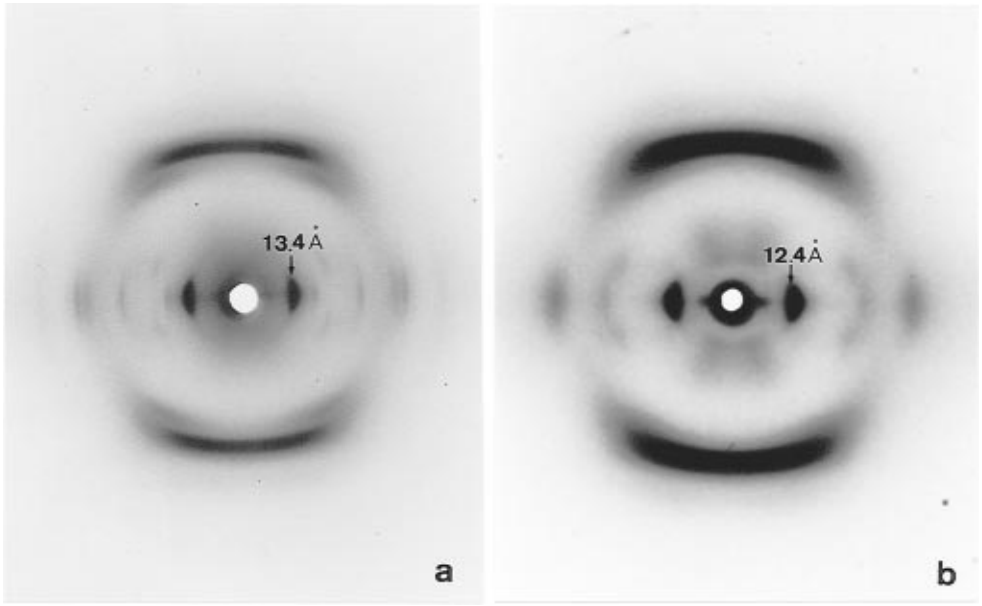

Figure 2. Fiber X-ray diffraction patterns of (a) poly(α-cyclohexyl-β-L-aspartate) and (b) poly(α-cyclopentyl-β-L-aspartate). Samples were oriented by stretching at 160 °C. The fiber axis is vertical in both cases.

packing energy was determined by considering the nonbonded interactions taking place between atoms contained in the monomeric units of the two central chains.

LALS Refinement. The crystal structure of PACHLA was refined by the linked-atom least-squares methodology against data obtained by X-ray diffraction from uniaxially oriented samples.[25] The averaged coordinates of the helix optimized by energy calculations were taken for building the initial models to be used for refinement. Bond lengths and angles were fixed at their standard values, the torsion angle ω was held in *trans*, and hydrogen bonds were assumed to be linear with an approximate length of 2.90 Å. The intensities of the X-ray reflections were measured with a Joyce-Loebl MK III CS microdensitometer. The integrated areas under each spot were corrected for orientation effects, and polarization and Lorentz factors were applied. No absorption correction was required since the films used for diffraction were very thin. Calculations were performed on a Silicon Graphics station RI-4000 and on an IBM-SP2 at the Centre de Supercomputació de Catalunya (CESCA).

Results and Discussion

X-ray Diffraction. Thin films of PACHLA obtained by casting from chloroform yielded poor Debye−Sherrer diagrams consisting of only a few diffuse rings. On the contrary, highly informative X-ray diffraction diagrams as that shown in Figure 2a could be obtained from fibers prepared by stretching at 160 °C. This diffractogram shows great resemblance to those reported for the hexagonal form of poly(β-L-aspartate)s bearing linear alkyl side chains of short and medium size;[5,6] remarkably similar features are the strong equatorial reflection at ∼13.5 Å, which is related with the side-by-side packing of the chains and the strong layer line at 4.5−5.0 Å corresponding to the pitch of a helix that contains four turns in the axial repeat. The diagram may be therefore interpreted on the basis of a structure composed of 13/4 helices with hydrogen bonds set between residues *i* and *i*+*3*. However the set of reflections placed along the equator cannot be indexed for a hexagonal structure as usually done for poly(β-L-aspartate)s in 13/4 helical conformation, but for a quasi-square lattice with lateral dimensions of 13.43 Å and 12.04 Å and an angle of 96°. In fact, a detailed inspection of the inner region of the equator revealed the presence of minor amounts of a reflection spacing about 12.0 Å, which is masked by the strong 13 Å reflection. The axial repeat is found to be 20.24 Å, which fits well within the range of values (19.9−21.0 Å) usually observed for the *c* parameter of the hexagonal form of poly(β-L-aspartate)s. Previous structural studies carried out on related compounds in the hexagonal form doubled the unit cell in order to include two chains in up-and-down arrangement. The result is a monoclinic lattice with the space group $P2_1$. In the case of PACHLA the situation is more complex because up to seven centered lattices differing in the arrangement followed by up-and-down chains may be generated. At this stage and in the absence of any diffraction evidence requiring a larger unit cell, the whole diagram has been preliminary indexed on the basis of a primitive oblique lattice of parameters $a_0 = 13.43$ Å, $b_0 = 12.04$ Å, $c_0 = 20.24$ Å, $\alpha = \beta = 90°$, and $\gamma = 96°$. Observed and calculated spacings for this structure are compared in Table 2. The density calculated is 1.31 g mL^{-1}, whereas the experimental value is 1.18 g mL^{-1}. Note that a discrepancy of 0.13 g mL^{-1} (which is less than 10%) is found, which may be perfectly acceptable if the partial crystalline nature of the sample and experimental errors are taken into account. It should be noted however that differences between experimental and calculated density values reported for other poly(β-L-aspartate)s exceptionally exceed 5%.

The fact that the hexagonal mode of packing characteristic of poly(β-L-aspartate)s arranged in 13/4 helical conformation has been abandoned in the case of PACHLA deserves some comments. Poly(α-*n*-octyl-β-L-aspartate) is the only member of the family that is known to crystallize in a nonhexagonal lattice made of 13/4 helices with lateral dimensions of $a_0 =$ 18.0 Å and $b_0 = 12.3$ Å.[8,10] In this case however the preference for a nonisometric mode of packing could be readily understood if the space distribution required by the polymer for accommodating the long alkyl groups is taken into account. In the case of PACHLA a similar explanation based on the size or shape of the side group would be not straightforward.

The X-ray diagram of a fiber of PACPLA prepared under the same conditions that were used in the case of PACHLA is shown in Figure 2b. The overall pattern is similar to that of PACHLA (Figure 2a), although it displays poorer definition,

TABLE 2: Observed and Calculated Spacings (Å) for the Fiber Patterns of Poly(α-cycloalkyl-β-L-aspartate)s

PACPLA (cyclopentyl)			PACHLA (cyclohexyl)			
d_{obsd}	hkl[a]	d_{calcd}	d_{obsd}	hkl[b]	hkl[c]	d_{calcd}
12.54	020, 110	12.44	13.32	100	100	13.36
6.22	040, 220	6.22	11.94	010	020	11.97
4.70	240, 310	4.70	9.41	−110	−120	9.42
4.10	060, 330	4.15	5.97	020	040	5.99
3.44	420	3.45	4.75	−120	−240	4.71
			4.41	−310	−320	4.32
			4.24	220	240	4.24
			3.71	−320	−340	3.77
				130	160	3.72
			3.27	400	400	3.34
10.66	021, 111	10.59	7.88	111	121	7.83
6.78	201, 131	6.76				
5.45	123	5.46	5.27	113	123	5.28
4.58	043, 223	4.56				
∼4.7	014	4.93	∼4.7		014	4.95
	104	4.75		104	104	4.73
	114, 024	4.67			−114	4.67
				014	024	4.66
					114	4.61
∼4.3	124	4.44	∼4.4	−114	−124	4.45
	034	4.30		114	124	4.34
∼4.0	005	4.03	∼3.9		015	3.99
	015	3.98		105	105	3.87

[a] Indexed for a monoclinic lattice with $a_0 = 14.37$ Å, $b_0 = 24.88$ Å, $c_0 = 20.14$ Å, $\alpha = \beta = \gamma = 90°$. [b] Indexed for a triclinic lattice with $a_0 = 13.43$ Å, $b_0 = 12.04$ Å, $c_0 = 20.24$ Å, $\alpha = \beta = 90°$, $\gamma = 96°$. [c] Indexed for a triclinic lattice with $a_0 = 13.43$ Å, $b_0 = 24.08$ Å, $c_0 = 20.24$ Å, $\alpha = \beta = 90°$, $\gamma = 96°$. In cases a and b the unit cell contains two chains in antiparallel arrangement.

indicating that a lower degree of order has been achieved. In this case the spacings measured on the equator are fully consistent with a hexagonal packing of chains separated by a distance of 14.4 Å. The original picture contains 12 reflections which can be accounted for by assuming a hexagonal unit cell of $a_0 = 14.37$ Å and $c_0 = 20.14$ Å but that has been indexed on the basis of an orthogonal lattice with parameters $a_0 = 14.37$ Å, $b_0 = 24.88$ Å, and $c_0 = 20.14$ Å by analogy with preceding related cases. Observed and calculated spacings for this structure are compared in Table 2. The unit cell in space group $P2_1$ contains two chains in 13/4 helical conformation that are oriented up−down to each other. The density calculated for this structure is 1.09 g mL^{-1}, which coincides with the value found experimentally. It is apparent that the crystal structure adopted by PACPLA follows suit the general pattern displayed by poly(β-L-aspartate)s with alkyl side chains of medium size (three and four carbon atoms).

Given the usual occurrence of polymorphs in poly(β-L-aspartate)s, we have searched further for other crystal forms in both PACHLA and PACPLA by preparing samples under those conditions known to favor the generation of either tetragonal or β-sheet structures.[9,11] Films obtained by evaporation from 2-chloroethanol did not contain traces of other crystal forms different from that found in films and fibers prepared from chloroform. On the other hand, no modification at all was detected in the X-ray diagrams of a hexagonal sample after annealing at 200 °C. These results are consistent with what could be expected from the size of the side groups since no conformation other than the 13/4 helix has been found up to date in poly(β-L-aspartate)s bearing alkyl groups larger than butyl.

Energy Calculations: Poly(α-cyclohexyl-β-L-aspartate). Firstly, a right-handed 13/4 helix with hydrogen bonds set between residues *i* and *i+3* was generated for a single chain of PACHLA. The helical geometry was optimized for each of the two alternative chair conformations assumable for the cyclohexyl side group, *i.e.* with the carboxyloxy group located at either the axial or the equatorial position. The conformational parameters and energies resulting from such calculations are shown in Table 3. A comparison of the individual energy terms for the two cases reveals grave distortions in the bond geometry of the axial conformer which are attributable to the existence of strong steric interactions among neighboring cyclohexyl side groups. The result is a surplus of energy of 7.9 kcal mol^{-1} residue^{-1} for the helix with the cyclohexyl group in axial conformation. In order to evaluate which would be the preferred conformation of the cyclohexyl ring if steric effects implying neighboring groups were removed, the contributions of the van der Waals and electrostatic energy terms for the two conformers have been calculated considering an isolated residue. It was found that both terms turn out to be unfavorable for the axial conformer, resulting in a total increment in the relative energy of about 1.4 kcal mol^{-1} residue^{-1}. In agreement with the results obtained previously in the conformational analysis of (*S*)-4-(cyclohexoxycarbonyl)-2-azetidinone[16] such energy excess would be attributable to the repulsive axial−axial 1,3 interactions operating in the axial conformer. Transversal and lateral views of the right-handed 13/4 helix of PACHLA with the cycloalkyl side group in equatorial conformation, as result from energy optimization, are shown in Figure 3.

In a second stage, the crystal structure of PACHLA was analyzed. For this, a set of 12 chains consisting of 18 residues in 13/4 helical conformation were placed in the oblique primitive lattice (13.43 × 12.04 Å, $\gamma = 96°$) determined by X-ray diffraction, and selected arrangements were subjected to molecular mechanics optimization. As depicted in Figure 4, two arrays, I and II, may be in principle assumed for placing the chains in the lattice depending whether successive layers are shifted by $\pm 1/2a$ or not. It should be noted that chain packing in array I is a slightly distorted hexagonal pattern, whereas array II is near to tetragonal. As mentioned above, several centered lattices are feasible for each array depending on what scheme of up-and-down chains is chosen for the antiparallel structure. Nevertheless, geometrical differences between some of them are so small that they turn out to be indistinguishable by either diffraction or theoretical methods. Therefore, we have confined the analysis to investigate the most relevant features of the crystal structure as they are (i) preference for array I or II, (ii)

TABLE 3: Torsional Angles and Energy Terms for a Single 13/4 Helical Chain of PACHLA Obtained by Energy Minimization

	torsional angles (deg)[a]						energy terms (kcal mol^{-1})[b]					
	main chain			side chain								
conformer	φ	ξ	ψ	ω	χ_1	χ_2	E_{bd}	E_{el}	E_{vdw}	Ehb	E_{tot}	ΔE
equatorial	154.6	−60.8	118.2	−178.2	179.3	−172.8	3.1	−62.3 (3.1)	−2.9 (−23.8)	−0.6	−62.7	0.0 (0.0)
axial	154.3	−60.0	118.0	180.0	179.1	49.6	11.6	−61.7 (3.5)	−4.0 (−22.8)	−0.6	−54.8	7.9 (1.4)

[a] The conformational angles correspond to those indicated in Figure 1. [b] Energy terms referred to one residue: E_{bd} = bonding energy, E_{el} = electrostatic energy, E_{vdw} = van der Waals energy, E_{hb} = energy corresponding to the $r^{-12}-r^{-10}$ term, E_{tot} = total energy, ΔE = relative difference energy. Figures in parentheses refer to one isolated residue so that interactions with neighboring side chains are neglected.

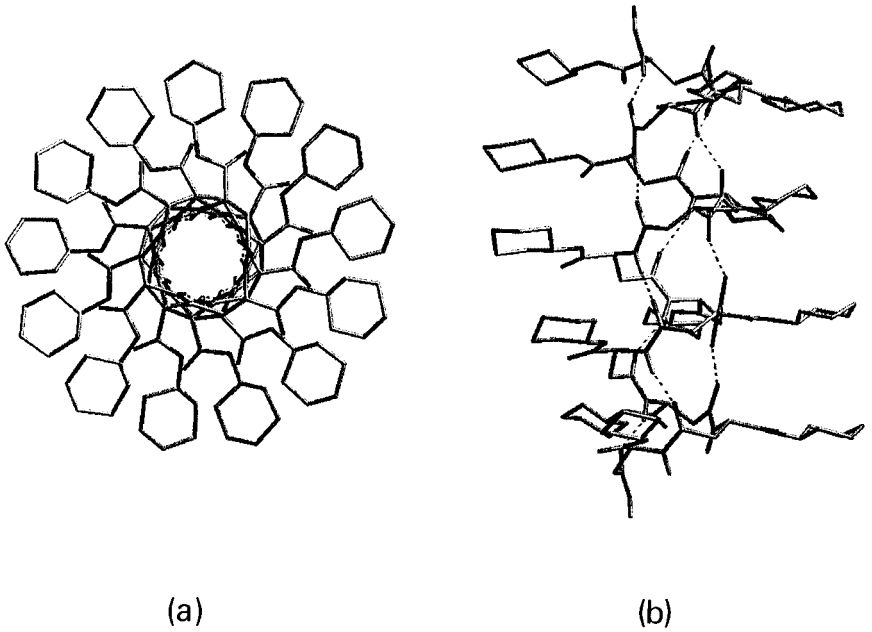

Figure 3. Axial (a) and equatorial projections (b) of a right-handed 13/4 helix of PACHLA obtained by energy minimization.

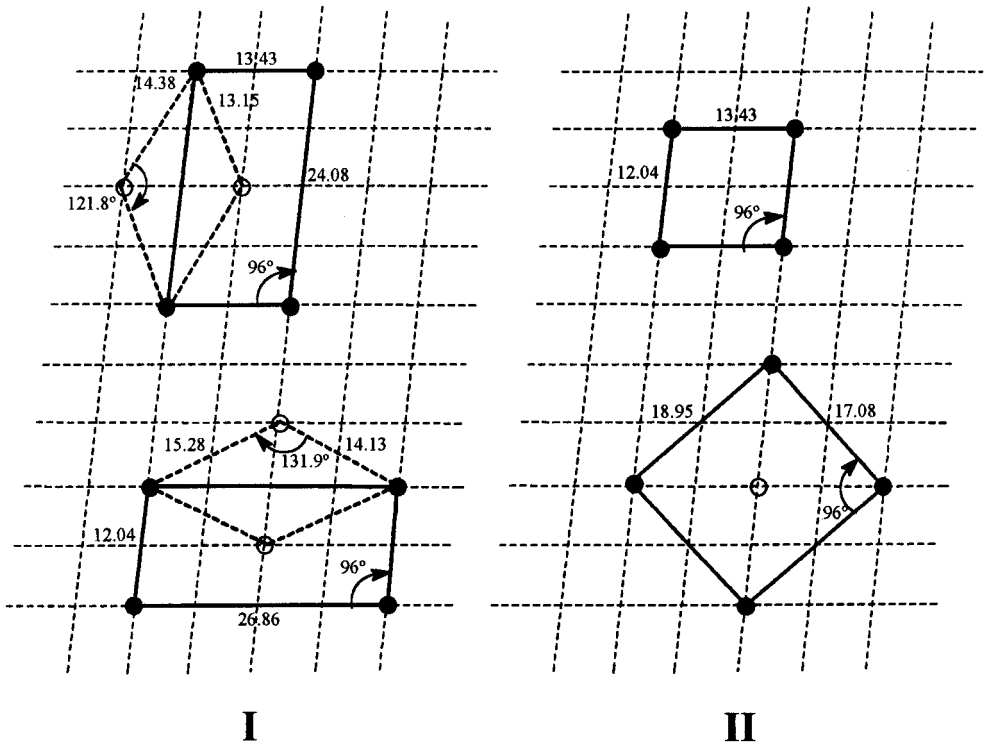

Figure 4. Schematic representation of different crystal models feasible for PACHLA: (I) quasi-hexagonal array (antiparallel models); (II) quasi-tetragonal array (parallel and antiparallel models).

relative orientation of the chains within the lattice, and (iii) chair conformation assumed by the cyclohexyl side group. Thus, both the parallel and antiparallel arrangements were examined for array I, and each one was tested for the cyclohexyl side group being in either axial or equatorial chair conformation. On the contrary, only the parallel model was considered in the analysis of array II since this is the arrangement occurring in poly(β-L-aspartate)s crystallized in the tetragonal form.

Results obtained for the four models considered for array I are compared in Table 4. The conformational parameters obtained for the 13 interior residues of the two central chains were used to provide the average torsion angles and energy values per residue. The up-and-down scheme selected for these calculations was that with the *b* axis doubled, resulting in a lattice of parameters $a_0 = 13.43$ Å, $b_0 = 24.08$ Å, $c_0 = 20.24$ Å, $\alpha = \beta = 90°$, and $\gamma = 96°$. Indexing of the X-ray pattern shown in Figure 2a made on the basis of this structure is given in Table 2. Comparison of data included in Table 4 leads us to conclude that the model consisting of an antiparallel packing of chains with the cyclohexyl side group in equatorial conformation is by far the most favored structure. Conformational parameters and energy term values resulting for such a model but with the *a* axis doubled instead of *b* turn out to be essentially the same. It is worthy to note that the equatorial conformer appears stabilized with respect to the axial one in an extent similar to that estimated for the isolated chain. This indicates the importance that intramolecular side group interactions have in the stabilization of the whole structure. Similar calculations

TABLE 4: Torsional Angles and Energy Terms for the Crystal Structure of PACHLA Obtained by Energy Minimization[a]

	torsional angles (deg)						energy terms (kcal mol^{-1})						H-bond geometry		
	main chain				side chain										
model	φ	ξ	ψ	ω	χ_1	χ_2	E_{bond}	E_{el}	E_{vdw}	E_{H-bond}	E_{tot}	ΔE	d(H···O) (Å)	d(N···O) (Å)	∠NHO (deg)
antiparallel															
equatorial	146.8	-59.1	129.2	-179.3	176.9	180.0	7.2	−60.5	−3.8	−0.2	−57.4	0.0	1.97	2.93	160.4
axial	146.3	-59.5	128.7	180.0	169.0	179.3	16.1	−62.0	−2.5	−0.4	−48.7	8.7	1.98	2.94	158.0
parallel															
equatorial	146.5	−59.5	128.9	−179.6	176.4	−165.2	9.7	−60.5	−3.8	−0.3	−54.6	2.7			
axial	146.4	−59.6	128.8	−179.9	171.1	134.1	14.4	−62.0	−2.5	−0.4	−52.0	5.3			

[a] For explanation of headings see footnote of Table 3.

TABLE 5: LALS Refinement of the Crystal Structure of PACHLA: Parallel and Antiparallel Models Compared

		parallel model $a_0 = 13.43$ Å, $b_0 = 12.04$ Å, $c_0 = 20.24$ Å $\alpha = \beta = 90°$, $\gamma = 96°$			antiparallel model (a axis doubled) $a_0 = 26.86$ Å, $b_0 = 12.04$ Å, $c_0 = 20.24$ Å $\alpha = \beta = 90°$, $\gamma = 96°$			antiparallel model (b axis doubled) $a_0 = 26.86$ Å, $b_0 = 12.04$ Å, $c_0 = 20.24$ Å $\alpha = \beta = 90°$, $\gamma = 96°$		
spot	F_{obs}	hkl	F_{calcd}	$\lvert F_{calcd} - F_{obs}\rvert$	hkl	F_{calcd}	$\lvert F_{calcd} - F_{obs}\rvert$	hkl	F_{calcd}	$\lvert F_{calcd} - F_{obs}\rvert$
1		010	189	189	010	27	27	020	20	20
2	286	100	217	69	200	213	73	100	217	69
3		110	64	64	210	6	6	120	4	4
4	58	−110	72		−210	55	3	−120	55	3
5	9	020	33	14	020	11	2	040	8	1
6	88	−220	136	24	−420	122	34	−240	123	35
7	154	220	129	26	420	159	5	240	160	6
		−310			−610			−320		3
8	195	130	121	74	230	156	39	160	155	9
		−320			−620			−340		
9	180	111	109	71	211	168	12	121	179	1
10	212	113	313	101	213	160	52	123	163	50
11	480	104	322	158	204	547	67	104	548	68
		−104			−204			−104		
		−114			−214			−124		

were then carried out for array II with chains arranged in parallel. Results revealed that this structure is destabilized in about 2 kcal mol^{-1} residue^{-1} when compared with the antiparallel model of array I.

Modeling and Refinement by LALS. The minimum energy model resulting from energy calculations, *i.e.* the antiparallel model with cyclohexyl side groups in equatorial conformation, was used to initiate the refinement of the crystal structure of PACHLA by LALS. Nine independent spots including about 16 reflections were used. Two imaginary spots corresponding to low indexed equatorial reflections absent in the X-ray diagram were also considered in the refinement. Firstly backbone dihedral angles were refined by applying contour conditions, and then the whole helical geometry including the conformation of the side chain was adjusted taking into account packing constraints and minimizing simultaneously intramolecular and intermolecular contacts. The agreement between observed and calculated intensities is good, resulting in an R factor of 17%, which may be well acceptable. However the overall refining process cannot be viewed as entirely satisfactory owing to the few X-ray data that can be used. Nevertheless the fact that the refined structure does not deviate significantly from that generated by energy calculations supports the reliability of the results. When refinement was repeated for the model with the a axis doubled instead of the b axis, the results were very similar and the R factor was 19%. On the contrary, discrepancies between calculated and observed intensities were found to be much more pronounced when the parallel model in array II was analyzed. In this case the resulting R factor was about 50%, revealing the inadequacy of the model. LALS results for the parallel and the antiparallel model are compared in Table 5, and dihedral angles, crystal parameters, and hydrogen bond geometry resulting for the antiparallel refined model of PACHLA, which can be considered as the most favored model for the crystal structure of this polymer, are shown in Table 6. A view of the projection of the unit cell down to the chain axis is shown in Figure 5.

TABLE 6: Crystal Structure of PACHLA: Conformational Parameters and Hydrogen Bond Geometry

helix symmetry	13/4 (right handed)
space group	$P1$
cell parameters	$a_0 = 13.43$ Å, $b_0 = 24.08$ Å, $c_0 = 20.24$ Å, $\alpha = \beta = 90°$, $\gamma = 96°$
torsional angles	
φ	145.2
ξ	−62.0
ψ	130.8
χ_1	−142.0
χ_2	−155.8
H−bond geometry	
d(H···O) (Å)	1.96
d(N···O) (Å)	2.89
∠NHO (deg)	155.2

NMR Measurements. NMR spectroscopy in this work has been used in this work with two purposes: firstly, to prove the occurrence of helices of PACPLA and PACHLA in solution. Secondly, the conformation of the side cyclohexyl group of PACHLA and its dependence on temperature are examined in both the liquid and solid states.

It is well-known that the familiar α-helix conformation of poly(α-amino acid)s is retained in solution provided that appropriate helicogenic solvents are used and that such conformation is readily disrupted by the action of strong acids. One of the most usual ways to follow the helix-to-random coil transition in polypeptides is to observe the changes taking place in the chemical shift of the proton attached to the α-carbon of the main chain. This procedure has been conveniently used to demonstrate the existence of such transition in certain poly(α-alkyl-β-L-aspartate)s[5,6] and poly(α-alkyl-γ-L-glutamate)s[26] by the effect of the addition of either trifluoroacetic or dichloroacetic acid.

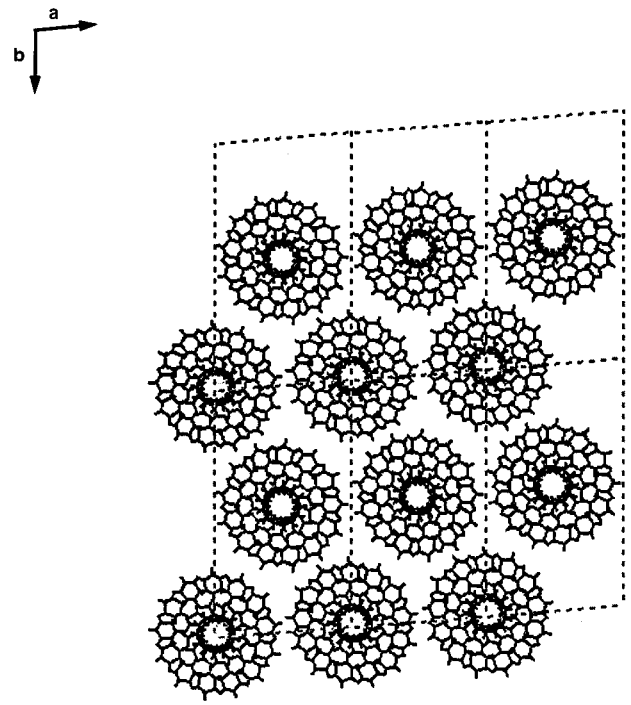

Figure 5. Projection of the quasi-hexagonal unit cell of PACHLA down the *c* axis for the model made of antiparallel chains with the *b* axis doubled. Separation between chains has been exaggerated to make clearer the representation.

Upon addition of trifluoroacetic acid, the chemical shift of the α-CH of PACHLA and PACPLA was observed to move high field from its initial value around 5.0 ppm to near 4.8 ppm. Simultaneously, the NH proton moves from 8.5 ppm up to near 7.9 ppm. The exact conditions used in these experiments as well as the precise signal displacements observed for both polymers are given in Table 7. The evolution of the ^{1}H NMR spectrum in the α-CH region when the concentration in trifluoroacetic acid increases from 0 to 3.0% is illustrated in Figure 6 for the case of PACHLA. It is apparent that the transition from helix to random coil takes place at TFA concentrations around 2−3% for both polymers, which is the range observed for poly(β-L-aspartate)s bearing linear alkyl side chains. These results reinforce preliminary conclusions drawn from earlier studies carried out on acyclic alkyl esters which pointed out that the stability of the 13/4 helix of poly(β-L-aspartate)s is essentially unaffected by the nature of the side group.

TABLE 7: ^{1}H NMR Data of the Helix−Coil Transition in Poly(α-cycloalkyl-β-L-aspartate)s

	δ (α-CH, in ppm)		δ (NH, in ppm)		% TFA (v/v)
polymer	helix[a]	coil[b]	helix[a]	coil[b]	(transition)
PACPLA	5.01	4.82	8.54	7.95	2.4
PACHLA	4.99	4.81	8.55	7.96	2.6

[a] In $CDCl_3$ with 0.4% of TFA. [b] In $CDCl_3$ with 3% of TFA.

The ^{13}C CP−MAS NMR spectra of a solid sample of PACHLA registered at 25, −70, and 80 °C are compared in Figure 7, and the corresponding chemical shift values measured in each case are listed in Table 8. Similar data for some related compounds previously studied by us have been included for

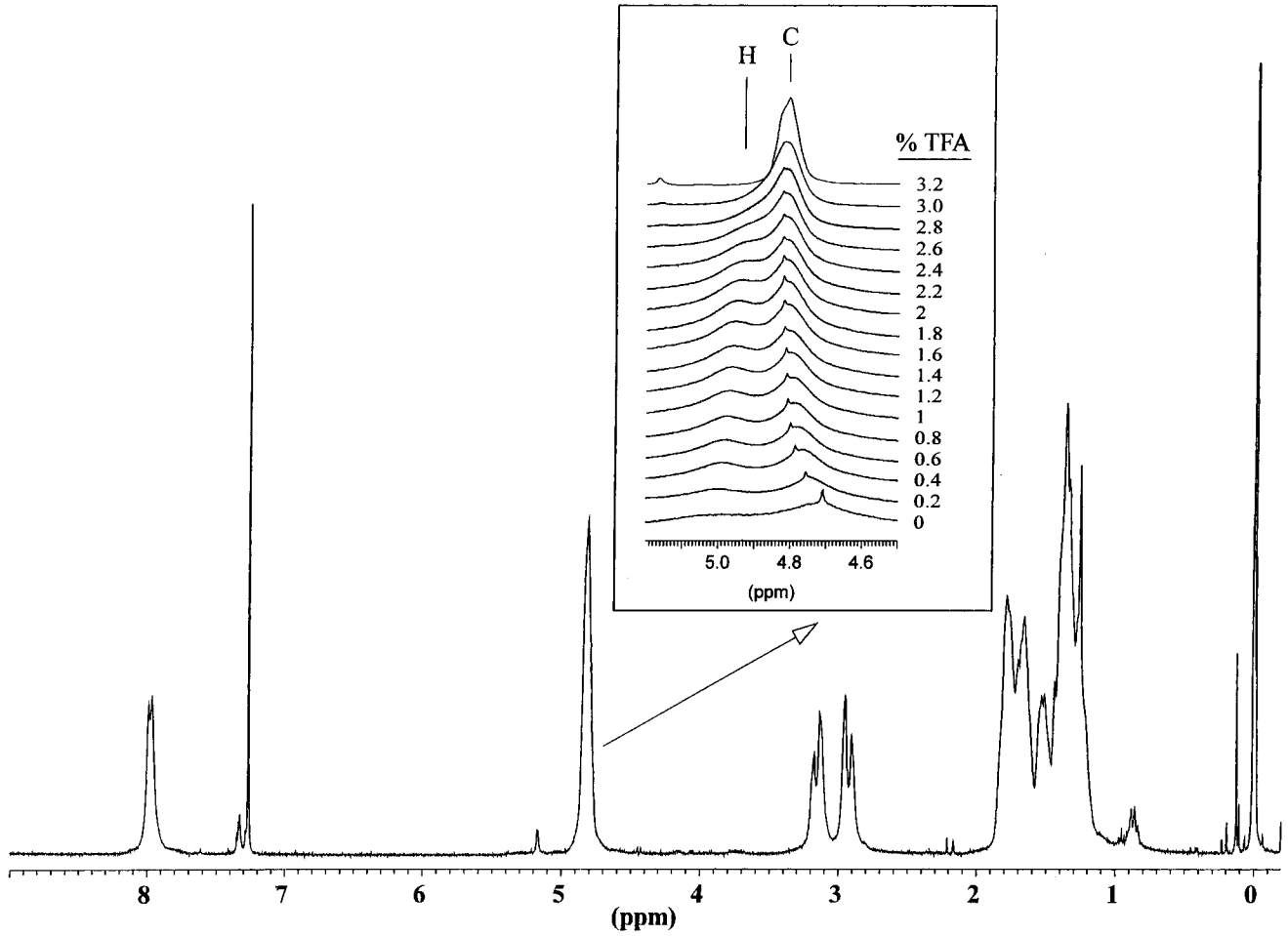

Figure 6. ^{1}H NMR (300.13 MHz) spectrum of PACHLA in CD_3Cl containing 5% (v/v) of trifluoroacetic acid. Inset: Displacement of the main chain CH signal with the TFA concentration (H, helical conformation; C, coil conformation).

TABLE 8: ^{13}C NMR Chemical Shifts (75.5 MHz) of PACHLA and (*S*)-4-(Cyclohexoxycarbonyl)-2-azetidinone

		main chain and ester side carbons (δ, ppm)				cyclohexyl carbons (δ, ppm)			
compound	T (°C)	C_α	C_β	HNCO	OCO	C_1	$C_{2,6}$	$C_{3,5}$	C_4
PACHLA (solid)	−70	37.4	48.8	sh[a]	170.4	74.0	31.8	26.7	26.7
	25	37.9	49.1	sh[a]	170.2	74.0	32.4	25.8	25.8
	80	37.5	49.1	sh[a]	170.1		31.6	25.9	25.9
PAALA-8 (solid)[b]	25	38.3	49.2	169.7	170.9				
azetidinone (solid)	25	44.2	47.5	169.4	171.6	76.4	32.1	26.9	26.9
azetidinone (solution)	25	43.5	47.5	166.7	170.5	74.4	31.4	23.6	25.2
	−63	43.3	47.3	167.7	171.0	75.2; 71.8[c]	31.5; 29.4[c]	24.2; 20.3[c]	25.6; 24.7[c]

[a] Shoulder of the ester peak. [b] Data for poly(α-*n*-octyl-*β*-L-aspartate) taken from López-Carrasquero *et al.*[8] [c] Two peaks corresponding to axial and equatorial conformers, respectively.

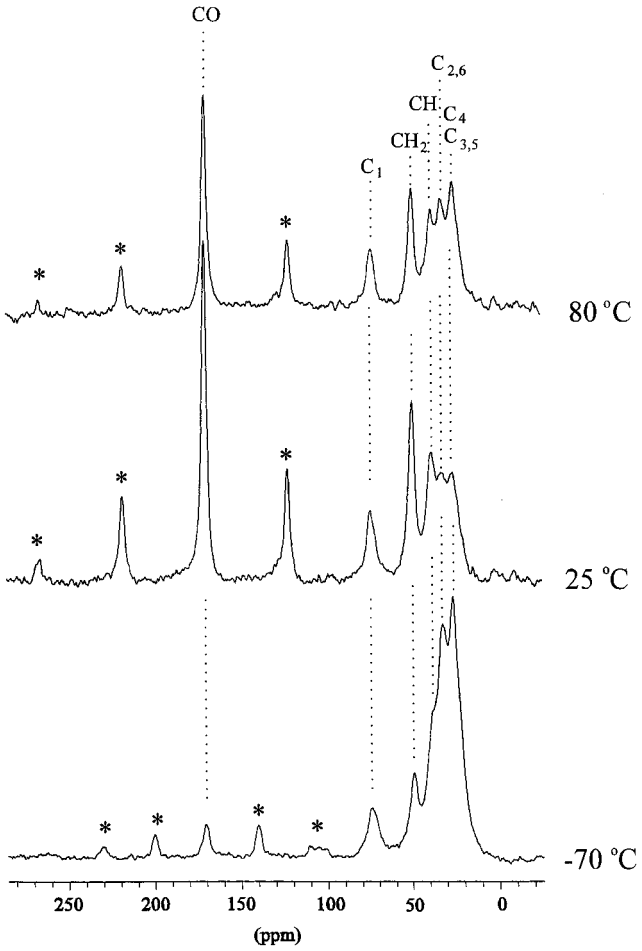

Figure 7. ^{13}C CP−MAS NMR (75.5 MHz) spectra of PACHLA at the indicated temperatures. *Spinning side bands.

comparison. The chemical shifts observed for the main chain carbons appear not to be affected by temperature, and their values are essentially the same as those reported for PAALA-8, a poly(*β*-L-aspartate) with an *n*-octyl side group that is known to be arranged in 13/4 helices.[8]

On the other side, the chemical shifts arising from the cyclohexyl carbons are not far from those observed for the same group in a crystalline sample of (*S*)-4-cyclohexoxycarbonyl-2-azetidinone, whose conformation has been proved to be equatorial. These signals are not affected by temperature changes, indicating the absence of variations in the conformational equilibrium of the cycle within the studied thermal interval. Comparison with the spectrum of the 2-azetidinone derivative registered in solution at −63 °C furnishes additional evidence in support of the exclusive existence of the equatorial conformer in solid PACHLA. At such temperature the chair equilibrium is nearly frozen and the two signals corresponding to the alternative axial and equatorial conformations appear separated by about 5 ppm. Such a difference in displacement is in the range usually observed for substituted cyclohexanes.[27] The similarity of the chemical shift values for the equatorial conformer to those observed for the cyclohexyl ring in PACHLA leaves no doubt about the equatorial preferences displayed by this group.

What is apparent in the spectra shown in Figure 7 is that peaks arising from side chain carbons become strengthened with regard to those arising from the main chain when temperature decreased to −70 °C. Increasing of intensity with temperature in CP−MAS NMR spectra is commonly attributed to a decreasing in the molecular motion, which favors the polarization transfer from the proton to the lattice. It may be concluded therefore that a second-order thermal transition implying a change in the dynamic of the side cyclohexyl group takes place in the proximity of −70 °C. In fact, preliminary dynamic mechanical measurements have revealed a remarkable damping in the surroundings of this temperature. The precise nature of such a transition is not clear however. In polycyclohexyl methacrylate the relaxation of the cyclohexyl units implying the flipping from one conformer to another is described to occur near −50 °C.[28,29] A similar mechanism could be invoked to account for the transition occurring in PACHLA. The fact that variations in chemical shifts of the cyclohexyl protons concomitant to the transition were not observed in the CP−MAS NMR spectra may be attributed to insufficient sensitivity of the technique to detect the small fraction of axial conformer presumably existing in this system.

Concluding Remarks

Several conclusions of interest in the pursuit of a detailed understanding of the structural behavior of poly(*β*-L-aspartate)s are drawn from the present study. First of all, the strong tendency shown by these polymers to be arranged in helices of characteristics similar to the familiar α-helix of poly(α-amino acid)s and proteins is corroborated. Although such a property has been evidenced before for a number of related compounds, this is the first time that the study is extended to poly(*β*-L-aspartate)s bearing cycloalkyl side chains. Whereas the helical conformation of the main chain is essentially unaffected, significant variations are introduced in the mode of packing of the chains in the case of the cyclohexyl derivative. Furthermore, energy calculations together with NMR experiments in solution have confirmed previous conclusions stating that the stability of the 13/4 helix is practically independent of the attributes of the side group. Finally, it has been shown also that the conformational equilibrium implying the axial−equatorial interconversion of the cyclohexyl side ring is completely unbalanced toward the conformer of lower energy both in solution and in the solid state. This is the result of the sum of two contributions, the unfavorable endocyclic 1,3 interactions

operating in the axial conformer and the side-by-side steric interactions taking place between neighboring residues in the 13/4 helix.

Acknowledgment. This research was supported by the Dirección General de Investigación Científica y Técnica (DGICYT) with Grant No. PB-93-0960. S.L. acknowledges the support of the Ministry of Education and Science of Spain for the award of a scholarship. The authors are indebted to the CESCA for computational facilities.

References and Notes

(1) Fernández-Santín, J. M.; Aymamí, J.; Rodríguez-Galán, A.; Muñoz-Guerra, S.; Subirana, J. A. *Nature (London)* **1984**, *311*, 53.
(2) Muñoz-Guerra, S. *Makromol. Chem., Macromol. Symp.* **1991**, *48/49*, 71.
(3) Muñoz-Guerra, S.; López-Carrasquero, F.; Rodríguez-Galán, A.; Fernández-Santín, J. M.; García-Alvarez, M.; Subirana, J. A. *Trends Macromol. Res.* **1994**, *1*, 181.
(4) Muñoz-Guerra, S.; López-Carrasquero, F.; Ferández-Santín, J. M.; Subirana, J. A. In *Encyclopedia of Polymeric Materials*; CRC Press: Boca Raton, FL, 1996; Vol 6, p 4694.
(5) Fernández-Santín, J. M.; Muñoz-Guerra, S.; Rodríguez-Galán, A.; Aymamí, J.; Lloveras, J.; Subirana, J. A.; Giralt, E.; Ptack, M.; *Macromolecules* **1987**, *20*, 62.
(6) López-Carrasquero, F.; Alemán, C.; García-Alvarez, M.; Martínez de Ilarduya, A.; Muñoz-Guerra, S. *Makromol. Chem. Phys*. **1995**, *196*, 253.
(7) López-Carrasquero, F.; Martínez de Ilarduya, A.; Muñoz-Guerra, S. *Polym. J.* **1994**, *26*, 694.
(8) López-Carrasquero, F.; Montserrat, S.; Martínez de Ilarduya, A.; Muñoz-Guerra, S. *Macromolecules* **1995**, *28*, 5535.
(9) López-Carrasquero, García-Alvarez, M.; Navas, J. J.; Alemán, C.; Muñoz-Guerra, S. *Macromolecules* **1996**, *29*, 8449.
(10) Alemán, C.; Navas, J. J.; López-Carrasquero, F.; Muñoz-Guerra, S. *Polymer*, in press.
(11) Muñoz-Guerra, S.; Fernández-Santín, J. M.; Alegre, C.; Subirana, J. A. *Macromolecules* **1989**, *22*, 1540.
(12) Bella, J.; Alemán, C.; Fernández-Santín, J. M.; Alegre, C.; Subirana, J. A. *Macromolecules* **1989**, *22*, 1540.
(13) Navas, J. J.; Alemán, C.; López-Carrasquero, F.; Muñoz-Guerra, S. *Macromolecules* **1995**, *28*, 4487.
(14) Ueno, A.; Takahashi, K., Anzai, J. U.; Osa, T. *J. Am. Chem. Soc*. **1981**, *103*, 6410.
(15) Pieroni, O.; Ciardelli, F. *Trends Polym. Sci*. **1995**, *3*, 282.
(16) León, S.; Martínez de Ilarduya, A.; Alemán, C.; García-Alvarez, M.; Muñoz-Guerra, S. *J. Phys. Chem. A* **1997**, *101*, 4208.
(17) García-Alvarez, M.; López-Carrasquero, F.; Tort, E.; Rodríguez-Galán, A.; Muñoz-Guerra, S. *Synth. Commun.* **1994**, *24*, 745.
(18) García-Alvarez, M.; Rodríguez-Galán, A.; Muñoz-Guerra, S. *Makromol. Chem. Rapid. Commun.* **1992**, *13*, 173.
(19) López-Carrasquero, F.; García-Alvarez, M.; Muñoz-Guerra, S. *Polymer* **1994**, *35*, 4502.
(20) Doty, P.; Bradbury, J. A.; Haltzer, A. M. *J. Am. Chem. Soc.* **1956**, *78*, 947.
(21) Weiner, S. J.; Kollman, P. A.; Case, D. A.; Singh, U. C.; Ghio, C.; Alagona, G.; Profeta, S.; Weiner, P. *J. Am. Chem. Soc.* **1984**, *106*, 765.
(22) Weiner, S. J.; Kollman, P. A.; Nguyen, D. T.; Case, D. A. *J. Comput. Chem.* **1986**, *7*, 230.
(23) Alemán, C.; Luque, F. J.; Orozco, M. *J. Comput. Aided Mol. Des.* **1993**, *7*, 721.
(24) Orozco, M.; Luque, F. J. *J. Comput. Chem.* **1990**, *11*, 909.
(25) Campbell-Smith, P. J.; Arnott, S. *Acta Crystallogr., Sect. A* **1978**, *34*, 3.
(26) Puiggali, J.; Muñoz-Guerra, S.; Rodríguez-Galán, A.; Alegre, C.; Subirana, J. A. *Makromol. Chem., Macromol. Symp.* **1988**, *20/21*, 167.
(27) Aliev, A. E.; Harris, D. M. *J. Am. Chem. Soc.* **1993**, *115*, 6369.
(28) Heijboer, J. *Kolloid Z.* **1956**, *134*, 149; *Ibid*. **1960**, *171*, 7.
(29) Lauprêtre, F.; Virlet, J.; Bayle, J.-P. *Macromolecules* **1985**, *18*, 1846.